2005 IEEE 61st Vehicular Technology Conference

VTC2005-Spring

STOCKHOLM

Paving the Path for a Wireless Future

Proceedings Volume 1 of 5

30 May—1 June 2005 Stockholm, Sweden

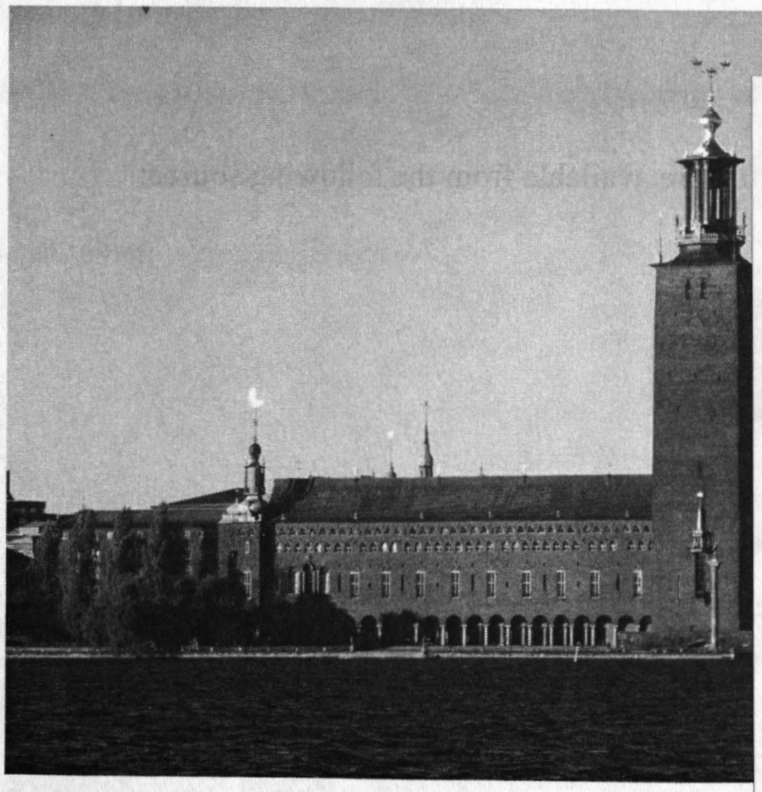

This book is due on the date indicated unless recalled by the Libraries. Books not returned on time are subject to replacement charges. Borrowers may access their library accounts at: http://www.lib.ncsu.edu/ads/borrow.html

IEEE

GOOGLE EXHIBIT 1010
Google v. Geoscope

2005 IEEE 61st Vehicular Technology Conference Proceedings

Copyright and Reprint Permission: Abstracting is permitted with credit to the source. Libraries are permitted to photocopy beyond the limits of U.S. Copyright law for private use of patrons those articles in this volume that carry a code at the bottom of the first page, provided the per-copy fee indicated in the code is paid through the Copyright Clearance Center, 222 Rosewood Drive, Danvers, MA 01923. For other copying, reprint, or republication permission, write to:

IEEE Copyrights Manager, IEEE Operations Center, 445 Hoes Lane, P.O. Box 1331, Piscataway, NJ 08855-1331.

All rights reserved. Copyright © 2005 by the Institute of Electrical and Electronics Engineers, Inc.

IEEE Catalog Number (Softbound): 05CH37631
IEEE Catalog Number (CD-ROM): 05CH37631C
ISSN: 1550-2252
ISBN Softbound: 0-7803-8887-9
ISBN CD-ROM: 0-7803-8888-7

Additional copies of this publication are available from the following source:

IEEE Operations Center
445 Hoes Lane
Piscataway, NJ 08854-4150 USA
+1 800 678 IEEE (+1 800 678 4333)
+1 732 981 1393
+1 732 981 9667 (FAX)
email: customer-service@ieee.org

Volume I

Antennas and Propagation

Channel Sounding, Evaluation, and Simulation

2-D DOA Estimation with Propagator Method for Correlated Sources Under Unknown Symmetric Toeplitz Noise 1
Nizar Tayem and Hyuck M. Kwon

L-Shape 2-Dimensional Arrival Angle Estimation with Propagator Method 6
Nizar Tayem and Hyuck M. Kwon

Joint Maximum Likelihood Estimation of Specular Paths and Distributed Diffuse Scattering 11
Andreas Richter and Reiner S. Thomä

A Novel MUSIC Algorithm for Direction-of-Arrival Estimation without the Estimate of Covariance Matrix and Its Eigendecomposition 16
Lei Huang, Shunjun Wu and Linrang Zhang

High Resolution Estimation of Directions of Arrival 20
Günes Z. Karabulut, Tolga Kurt and Abbas Yongacoglu

Nominal Direction and Direction Spread Estimation for Slightly Distributed Scatterers Using the SAGE Algorithm 25
Xuefeng Yin and Bernard H. Fleury

Channel Models

A Multi-Wall Path Loss Model for Indoor UWB Propagation 30
Annalisa Durantini and Dajana Cassioli

Assessment of a New Indoor Propagation Prediction Method Based on a Multi-Resolution Algorithm 35
Katia Runser and Jean-Marie Gorce

A Generic Narrowband Model for Radiowave Propagation Through Vegetation 39
Jürgen Richter, Rafael F. S. Caldeirinha, Miqdad O. Al-Nuaimi, Andy Seville, Neil C. Rogers and Nick Savage

A Simple Efficient Method for Generating Independent Nakagami-m Fading Samples 44
Lingzhi Cao and Norman C. Beaulieu

A Framework for Analysis of Antenna Effects in UWB Communications 48
Alain Sibille

Empirical Comparison of MIMO Antenna Configurations 53
Pasi Suvikunnas, Jari Salo, Jarmo Kivinen and Pertti Vainikainen

Statistical Channel Models 1

A Modified S-V Clustering Channel Model for the UWB Indoor Residential Environment 58
Chia-Chin Chong, Youngeil Kim and Seong-Soo Lee

A Statistical Mobile-to-Mobile Rician Fading Channel Model 63
Li-Chun Wang and Yun-Huai Cheng

Statistical Analysis of Measured Radio Channels for Future Generation Mobile Communication Systems 68
Mathias Riback, Henrik Asplund, Jonas Medbo and Jan-Erik Berg

Comparison of Empirical Propagation Path Loss Models for Fixed Wireless Access Systems 73
V. S. Abhayawardhana, I. J. Wassell, D. Crosby, M. P. Sellars and M. G. Brown

Statistical Modelling of a Radio Propagation Channel in an Underground Mine at 2.4 and 5.8 GHz 78
Mathieu Boutin, Sofiène Affes, Charles Despins and Tayeb Denidni

Small-Scale Fading Prediction Using an Artificial Neural Network 82
Erik Östlin, Hans-Jürgen Zepernick and Hajime Suzuki

Statistical Channel Models 2

Distribution of the Amplitude of a Sum of Singly and Doubly Scattered Fading Radio Signal 87
Jari Salo, Jussi Salmi and Pertti Vainikainen

Indoor/Outdoor Location of Cellular Handsets Based on Received Signal Strength 92
Jian Zhu and Gregory D. Durgin

Propagation Characteristics of IEEE 802.15.4 Radio Signal and Their Application for Location Estimation 97
Shinsuke Hara, Dapeng Zhao, Kentaro Yanagihara, Jumpei Taketsugu, Kiyoshi Fukui, Shigeru Fukunaga and Ken-ichi Kitayama

Modelling of Propagation Environments Inside a Scattered Field Chamber 102
Magnus Otterskog

Time Variability of the Foliated Fixed Wireless Access Channel at 3.5 GHz 106
D. Crosby, V. S. Abhayawardhana, I. J. Wassell, M. G. Brown and M. P. Sellars

Calibration of an Indoor Radio Propagation Prediction Model at 2.4 GHz by Measurements of the IEEE 802.11b Preamble 111
Jaouhar Jemai, Radoslaw Piesiewicz and Thomas Kürner

MIMO Channel Models 1

Capacity of Diagonally Correlated MIMO Channels 116
Hüseyin Özcelik and Claude Oestges

Macrocellular Directional Channel Modeling at 1.9 GHz: Cluster Parameterization and Validation 121
Claude Oestges, Danielle Vanhoenacker-Janvier and Bruno Clerckx

MIMO Channel Capacity Modeling Using Markov Models 126
S. Vaihunthan, S. Haykin and M. Sellathurai

Space-Time Correlation for Narrow- and Wideband MIMO Fading Signals in Macro- and Microcells 131
Po-Ying Chen and Hsueh-Jyh Li

Correlation Matrix Distance, a Meaningful Measure for Evaluation of Non-Stationary MIMO Channels 136
Markus Herdin, Nicolai Czink, Hüseyin Özcelik and Ernst Bonek

Effect of Random Walk Phase Noise on MIMO Measurements 141
Peter Almers, Shurjeel Wyne, Fredrik Tufvesson and Andreas F. Molisch

MIMO Channel Models 2

Statistical Evaluation of Outdoor-to-Indoor Office MIMO Measurements at 5.2 GHz 146
Shurjeel Wyne, Andreas F. Molisch, Peter Almers, Gunnar Eriksson, Johan Karedal and Fredrik Tufvesson

Diversity and Correlation in Rayleigh Fading MIMO Channels 151
Michel T. Ivrlac and Josef A. Nossek

What Makes a Good MIMO Channel Model? 156
Hüseyin Özcelik, Nicolai Czink and Ernst Bonek

Spatial and Polarization Characterization of MIMO Channels in Rural Environment 161
Dmitry Chizhik, Jonathan Ling, Dragan Samardzija and Reinaldo A. Valenzuela

Capacity Analysis for Compact MIMO Systems 165
B. K. Lau, S. M. S. Ow, G. Kristensson and A. F. Molisch

MIMO Channel Measurements for Personal Area Networks 171
Anders J. Johansson, Johan Karedal, Fredrik Tufvesson and Andreas F. Molisch

Smart Antennas and MIMO Systems 1

Performance of Different Interpolation Strategies for an OFDM/MMSE Smart Antenna System in an Indoor WLAN . 177
Karim M. Nasr, Fumie Costen and Stephen K. Barton

Reverse Link Capacity of CDMA Systems with Imperfect Beamforming Using Different Types of Antenna Arrays ... 182
Jin Yu and Yu-Dong Yao

Compact Feedback for MIMO-OFDM Systems over Frequency Selective Channels 187
Qinghua Li and Xintian Eddie Lin

Lattice Array Receiver and Sender for Spatially OrthoNormal MIMO Communication 192
Peter Larsson

Spatio-Diversity Estimate of a System-Dependent Wideband Directional Channel 197
Yifan Chen and Vimal K. Dubey

Random Beamforming in MIMO Systems Exploiting Efficient Multiuser Diversity 202
Eun Yong Kim and Joohwan Chun

Smart Antennas and MIMO Systems 2

Antenna Selection for MIMO Systems Based on an Accurate Approximation of QAM Error Probability 206
Fatma Kharrat-Kammoun, Sandrine Fontenelle, Stéphanie Rouquette and Joseph J. Boutros

QoS-Based User Scheduling for Multiuser MIMO Systems 211
Marios Kountouris, Ashish Pandharipande, Hojin Kim and David Gesbert

Random Unitary Beamforming with Partial Feedback for Multi-Antenna Downlink Transmission Using Multiuser Diversity 216
Haibo Wang, Alex B. Gershman and Thia Kirubarajan

Channel Estimation in MIMO OFDM Systems with Sparse Pilot Tones 221
Sugbong Kang and James S. Lehnert

A Dual Band Back Coupled Meanderline Antenna for Wireless LAN Applications 226
A. Khaleghi, A. Azoulay and J. C. Bolomey

System Comparison of Smart and Dumb Antennas 230
Mats Bengtsson, Patrick Svedman, Xi Zhang and Per Zetterberg

Antennas and Propagation Posters

Mobile Antenna System for Ku-Band Satellite Internet Service 234
Seong Ho Son, Ung Hee Park, Soon Ik Jeon and Chang Joo Kim

Evaluation of the Bluetooth Link and Antennas Performance for Indoor Office Environments by Measurement Trials and FEMLAB Simulations 238
Abbas Mohammed and Tommy Hult

Continuous State HMM Modeling of Flat Fading Channels 243
William Turin and Rittwik Jana

Field Measurement Based Performance Analysis of Digital Audio Broadcasting (DAB) Reception in Mobile Channels 247
M. Velez, D. de la Vega, P. Angueira, D. Guerra, G. Prieto and A Arrinda

Analysis and Measurements for Indoor Polarization MIMO in 5.25 GHz Band 252
Jyri Hämäläinen, Risto Wichman, Jukka-Pekka Nuutinen, Juha Ylitalo and Tommi Jämsä

Evaluation of Diversity Antenna Characteristics in Narrow Band Fading Channel Using Random Phase Generation Process 257
A. Khaleghi, A. Azoulay and J. C. Bolomey

Transmission Technology

CDMA Systems 1

On the Impact of Imperfect Multipath Detection on the Performance of CDMA Systems with Space-Time Spreading. 262
Mohamed Abou-Khousa, Ali Ghrayeb and Mohamed El-Tarhuni

Digital Image Signal Rejection in WCDMA Receivers Based on Adaptive Interference Cancellation 267
Mikko Valkama, Lauri Anttila and Markku Renfors

An Iterative Frequency-Domain Decision-Feedback Receiver for MC-CDMA Schemes 271
Rui Dinis, Paulo Silva and Antonio Gusmão

A 2D Space-Frequency Receiver with Reduced-Rank Multistage Wiener Filters for MC-CDMA Systems 276
Yung-Fang Chen and Chung-Hung Wang

Combined Spatial Multiplexing and Diversity Techniques for Coded MC-CDMA Systems with Suboptimal MMSE-Based Receivers 280
Mikko Vehkaperä, Djordje Tujkovic, Zexian Li and Markku Juntti

Reduced Complexity Joint Detection Generalized RAKE Receiver for WCDMA MIMO Systems 285
Stephen J. Grant and Karl J. Molnar

CDMA Systems 2

Maximizing Throughput Using HSDPA with MIMO in UMTS Macro-Cell Environment 290
P. Vieira, M. P. Queluz and A. Rodrigues

Joint Optimization of Radio Parameters in HSDPA 295
B. Zerlin, M. Ivrlac, W. Utschick, J. Nossek, I. Viering and A. Klein

Adaptive Multistage Detection for DS-CDMA Systems in Multipath Fading Channels 300
Min Li and Walaa Hamouda

MAI-Minimized Signature Waveforms for MC-DS-CDMA Systems 305
S. Sureshkumar, E. Shwedyk and Ha H. Nguyen

Coded CDMA in Cooperative Channels 310
Ebrahim Karami, Mohsen Shiva and Mohammad Abtahi

3G

Power Control and Utility Optimization in Wireless Communication Systems 314
Dimitrie C. Popescu and Anthony T. Chronopoulos

Resource Allocation in HSDPA Using Best-Users Selection Under Code Constraints 319
Ghassane Aniba and Sonia Aïssa

Efficient and Fair Scheduling for Best-Effort Downlink Packet Data 324
Dong In Kim

Cost Analysis of Smart Antenna Systems Deployment 329
Andres Alayon Glazunov, Peter Karlsson and Rickard Ljung

HSDPA Link Adaptation Based on Novel Quality Model 334
Wang Hai, Wan Lei and Liao Min

Utilizing Code Orthogonality Information for Interference Suppression in UTRA Downlink 339
Mythri Hunukumbure, Mark Beach and Julian Webber

On Closed Loop Transmit Diversity for HSDPA - Using an Orthogonality Matrix for System Level Evaluations 344
Markus Ringström, David Astély and Bo Göransson

Closed Loop Transmit Diversity in WCDMA HS-DSCH 349
Afif Osseiran and Andrew Logothetis

Other-Cell Interference in the Downlink of Multi-Service UMTS 354
S.-E. Elayoubi, B. Elsaghir and T. Chahed

Steered Optimization Strategy for Automatic Cell Planning of UMTS Networks 359
Sana Ben Jamaa, Zwi Altman, Jean-Marc Picard and Arturo Ortega

(Re)Active Load Control Based on Radio Link Quality for the UMTS/WCDMA Forward Link 363
Emanuel B. Rodrigues, Francisco R. P. Cavalcanti, Carlos H. M. de Lima and Vicente A. de Sousa Jr.

On the Enhancement of Monte Carlo 3G Network Modelling Tools for QoS Prediction 368
Benoît Fourestié and Sylvain Renou

CDMA

Noncoherent Digital Delay-Lock Loops for Direct-Sequence Spread-Spectrum Signals Over Weibull Fading Channels 372
Tsan-Ming Wu and Chung-Hua Chuang

Performance Benefits of Fractional Sampling in the Initial Code Synchronization for the Wireless Access of 3G Mobile Communications 377
Francesco Benedetto, Marco Carli, Gaetano Giunta and Alessandro Neri

SINR for DS-CDMA with Random Spreading 382
Ping-Hung Chiang, Ding-Bing Lin and Hsueh-Jyh Li

Performance Evaluation of Interleaved MC-CDMA Systems with Correlated Nakagami-m Fading Channels 387
Zexian Li and Matti Latva-aho

UCHT Complex Sequences for Downlink Multi-Carrier DS-CDMA Systems 392
Zhenghui Gu, Shoulie Xie and Susanto Rahardja

Generalized Decorrelating Discrete-Time RAKE Receiver 396
Tunçer Baykas, Mohamed Siala and Abbas Yongacoglu

Optimal Number of Rake Combiners for Multiple Codes Assignment with Fast Handoff in UMTS Mobile Networks 401
Ben-Jye Chang

STBC Site Diversity for Multicarrier CDMA in Linear Cell System 406
Takeo Fujii, Yukihiro Kamiya and Yasuo Suzuki

Distributions of Orthogonality Factor and Multipath Gain of the UMTS Downlink Obtained by Measurement Based Simulations 411
Heinz Droste and Jürgen Beyer

W-CDMA Uplink Soft Handover Gain Measurements 416
Mario Da Silva and Yann Farmine

Location Dependent CDMA Orthogonality in System Level Simulations 419
S. Burger, H. Buddendick, G. Wölfle and P. Wertz

Total Weighted Square Correlation of Multipath Multibase Synchronous DS-CDMA Systems 424
Paul Cotae, Zorica Pantic-Tanner and Matt Aguirre

Channel Estimation and Equalization 1

Estimation of the Channel Impulse Response Length and the Noise Variance for OFDM Systems 429
Van Duc Nguyen, Hans-Peter Kuchenbecker and Matthias Pätzold

Joint ML Channel Estimation and Data Detection for STBC via Novel Sphere Decoding Algorithms 434
Weiyu Xu, Youzheng Wang, Zucheng Zhou and Jing Wang

A Faster ML Sphere Decoder with Competing Branches 438
Anxin Li, Weiyu Xu, Youzheng Wang, Zucheng Zhou and Jing Wang

Impact of Imperfect Channel Estimation on OFDM/TDM Performance 442
Shinsuke Takaoka, Haris Gacanin and Fumiyuki Adachi

Pilot-Assisted Channel Estimation Based on MMSE Criterion for DS-CDMA with Frequency-Domain Equalization 447
Kazuaki Takeda and Fumiyuki Adachi

Multi-Antenna Pre-Equalization for Single-Carrier/TDD System 452
Fumiyuki Adachi, Kazuaki Takeda and Hiromichi Tomeba

Channel Estimation and Equalization 2

UMTS FDD Frequency Domain Equalization Based on Slot Segmentation 457
Yushan Li, Steve McLaughlin and David G. M. Cruickshank

Reduced Search Space Scheme for Detection of Spatial Division Multiplexing 462
Heejung Yu, Taehyun Jeon and Sok-Kyu Lee

Joint Channel Estimation and Phase Noise Suppression for OFDM Systems 467
Jong-Ho Lee, Jun-Seok Yang, Seong-Cheol Kim and Yong-Wan Park

Iterative Channel Estimation for MC-CDMA 471
Stephan Sand, Ronald Raulefs and Gunther Auer

Iterative B-Spline Channel Estimation for Space-Time Block Coded Systems in Fast Flat Fading Channels 476
Huiheng Mai, Yuriy V. Zakharov and Alister G. Burr

Performance Evaluation of Frequency Domain Equalization and Channel Estimation for Direct Sequence - Ultra Wideband (DS-UWB) System 481
Hiroyuki Sato and Tomoaki Ohtsuki

Channel Estimation and Equalization 3

On Low Complexity ML Detection Algorithm in MIMO System 486
Hongwei Zhang, Haibin Zhang, Hanwen Luo and Wentao Song

MMSE Channel Estimation Using Two-Dimensional Filtering in Rapid Time-Variant Environments 490
Gabriele Donà and Witold A. Krzymien

Sparse Channel Estimation for OFDM Transmission Based on Representative Subspace Fitting 495
Chun-Jung Wu and David W. Lin

Joint Channel and Carrier Offset Estimation in an Asynchronous CDMA System 500
Hongyi Fu and Samir Attallah

Outage-Based LDPC Code Design for SC/MMSE Turbo-Equalization 505
Rainer Wohlgenannt, Kimmo Kansanen, Djordje Tujkovic and Tad Matsumoto

DFT-Based PSA Channel Estimation Using Linear Prediction for OFDM Systems with Virtual Carriers 510
Jeong-Wook Seo, Jung-Wook Wee, Yong-Suk Park, Jong-Ho Paik and Won-Gi Jeon

Channel Estimation and Equalization 4

Blind Iterative Channel Estimation and LDPC Decoding for OFDM Systems 514
Mi-Kyung Oh, Yeong-Hyeon Kwon, Jung-Hyun Park and Dong-Jo Park

Iterative Channel Equalization, Channel Decoding and Source Decoding 518
Jin Wang, Lie-Liang Yang and Lajos Hanzo

Approximate Best Linear Unbiased Channel Estimation for Frequency Selective Channels with Long Delay Spreads: Robustness to Timing and Carrier Offsets 523
Serdar Özen, S. M. Nerayanuru, Christopher Pladdy and Mark J. Fimoff

Generic Reduced-Complexity MMSE Channel Estimation for OFDM and MC-CDMA 528
J. Akhtman and L. Hanzo

Iterative MLD Equalizer Preceded by MIMO-FDE for Wideband Spatial Multiplexing Systems 533
Yasunori Nouda, Toshiaki Koike and Susumu Yoshida

Single Sideband QPSK with Turbo Equalization for Mobile Communications 538
Boonsarn Pitakdumrongkija, Hiroshi Suzuki, Satoshi Suyama and Kazuhiko Fukawa

Channel Estimation and Equalization 5

Wideband Channel Estimation and Prediction in Single-Carrier Wireless Systems 543
Wei Liu, Lie-Liang Yang and Lajos Hanzo

A Pilot-Assisted Equalisation Scheme for the UMTS-TDD Downlink with Partial Loading 548
Mahmoud Hadef and Stephan Weiss

Adaptive Channel SVD Estimation for MIMO-OFDM Systems 552
H. Zamiri-Jafarian and G. Gulak

A Velocity-Adaptive Channel Estimation Scheme Using the Simple Zero-Forcing Technique in the Frequency Domain 557
Takki Yu, Goohyun Park, Daesik Hong and Changeon Kang

Blind Identification and Equalization of LDPC-Encoded MIMO Systems 562
Ansgar Scherb, Volker Kühn and Karl-Dirk Kammeyer

Novel SMC Techniques for Blind Equalization of Flat-Fading MIMO Channels 567
Manuel A. Vázquez, Joaquín Míguez and Mónica F. Bugallo

Coding and Modulation 1

Performance Analysis of a Trellis Coded Beamforming Scheme for MIMO Fading Channels 572
L. Chu and J. Yuan

Performance Analysis of M-ary PSK Adaptive Modulation System Over Rayleigh-Lognormal Fading Channel 576
Hsin-Piao Lin, Ming-Chien Tseng and Ding-Bing Lin

Multi-Dimensional MPSK for Iterative Demapping Over AWGN and Rayleigh Fading Channels 581
Xin Qi, Ming Zhao, Shidong Zhou and Jing Wang

A New Labeling Search Method for Bit-Interleaved Coded Modulation with Iterative Decoding 587
Qi Cheng, Xibin Xu, Shidong Zhou and Limin Xiao

High Girth LDPC Codes Construction Based on Combinatorial Design 591
Fan Zhang, Ying Xu, Xuehong Mao and Wuyang Zhou

A Novel TCM-Based Hybrid ARQ for Efficient Bandwidth Utilization 595
Qian Huang, Sammy Chan, Li Ping, King-Tim Ko and Moshe Zukerman

Coding and Modulation 2

Performance of Finite-Depth Interleaved Convolutional Codes in a Rayleigh Fading Channel with Noisy Channel Estimates 600
Jittra Jootar, James R. Zeidler and John G. Proakis

Low Complexity Stopping Criterion for LDPC Code Decoders 606
Frank Kienle and Norbert Wehn

Throughput of Turbo Coded Hybrid ARQ Using Single-Carrier MIMO Multiplexing 610
Akinori Nakajima, Deepshikha Garg and Fumiyuki Adachi

Parallel Iterative Decoding for Orthogonal Convolutional Codes 615
Yu-Cheng He, David Haccoun and Christian Cardinal

Flexible Channel Feedback Quantization in Multiple Antenna Systems 620
Bartosz Mielczarek and Witold Krzymien

Joint Source-Channel Decoding of Correlated Sources Over ISI Channels 625
Javier Del Ser, Pedro Crespo and Arrate Muñoz

Coding and Modulation 3

Generalized PSK for Improved Iterative Decoding and Demodulation of Coded DPSK Systems 630
Frieder Sanzi and Marc C. Necker

Lowering Error Floors of Irregular LDPC Code on Fast Fading Environment with and without Perfect CSI 634
Satoshi Gounai and Tomoaki Ohtsuki

Multirate Diagonal-Space-Time-Interleaved Coded Modulation for Non-Ergodic Block Fading Channels 639
Mathini Sellathurai

Delta Modulation for Channel Feedback in Transmit Diversity Systems 644
Havish Koorapaty, Leonid Krasny and R. Ramésh

Adaptive Coding for OFDM Based Systems Using Generalized Concatenated Codes 649
Omar Al-Askary, Lazaros Sidiropoulos, Lukas Kunz, Christos Vouzas and Chafic Nassif

Code Optimization with Serially Concatenated Trellis Coded Modulation on a Fading Channel 654
Asgeir Nysæter

Coding and Modulation 4

Coded Spreading with m-Sequences 659
Ozgur Ekici

On the Threshold of Right Regular LDPC Codes for the Erasure Channel 664
Enrico Paolini and Marco Chiani

Hierarchical Subgroup Power and Modulation Coding Adaptation: A New Frequency-Space Link Adaptation Scheme in MIMO-OFDM Eigenmode Adaptive Transmission System 668
Le Hai Doan, SeeHo Ting, Kei Sakaguchi and Kiyomichi Araki

Improved Decoding with the Bi-Directional SOVA for Turbo Codes 673
Yu-Chuan Chang and Jenn-Kaie Lain

A Linear Criterion to Optimize Irregular LDPC Codes for OFDM Communications 678
Valérian Mannoni, Guillaume Gelle and David Declercq

Bit-to-Symbol Mapping in LDPC Coded Modulation 683
Yuan Li, Chin Keong Ho, Yan Wu and Sumei Sun

Decoding 1

The Box-Minus Operator and its Application to Low-Complexity Belief Propagation Decoding 687
Thorsten Clevorn and Peter Vary

Slab-Sphere Decoding: Efficient Maximum-Likelihood Detection for Asymmetric MIMO Antenna Systems 692
Kai-Kit Wong, Arogyaswami Paulraj and Ross D. Murch

List Slab-Sphere Decoding: Efficient High-Performance Decoding for Asymmetric MIMO Antenna Systems 697
Kai-Kit Wong, Arogyaswami Paulraj and Ross D. Murch

Reduced Memory Turbo MAP Decoding Algorithm for Non-Binary Orthogonal Signaling 702
Dae-Son Kim, Young-Joon Kim and Hong-Yeop Song

A New LDPC Decoding Algorithm Aided by Segmented CRCs for Erasure Channels 705
Yeong-Hyeon Kwon, Mi-Kyung Oh and Dong-Jo Park

Reliability Ratio Based Weighted Bit-Flipping Decoding for LDPC Codes 709
Feng Guo and Lajos Hanzo

Volume II

Decoding 2

Low Complexity Decoding of BICM STBC 715
Enis Akay and Ender Ayanoglu

Analysis of a Sub-Block Recovery Scheme for Decoding a Concatenated Error Control Code 719
Chunlong Bai, Witold A. Krzymien, Ivan J. Fair and Bartosz Mielczarek

Soft Decision Metrics for Turbo-Coded FH M-FSK Ad Hoc Packet Radio Networks 724
B. M. Peric, M. R. Souryal, E. G. Larsson and B. R. Vojcic

Fast Finger Selection for GRAKE 728
Ali S. Khayrallah and Douglas A. Cairns

Multi-Dimensional Mapping for Bit-Interleaved Coded Modulation 733
Frederik Simoens, Henk Wymeersch and Marc Moeneclaey

On the Joint Detection SAIC Algorithm in Asynchronous GSM Network 738
Zhigang Tian, Wenbin Guo and Dacheng Yang

Equalisation and Estimation

Joint LMMSE Equalizer for HSDPA in Full-Rate Space Time Transmit Diversity Schemes 743
Domenico Giustiniano, Stefano Mangione, Giovanni Garbo and Giuseppe Avellone

Frequency-Domain Pre-Equalization Transmit Diversity for DS-CDMA Mobile Radio 748
Hiromichi Tomeba, Kazuaki Takeda and Fumiyuki Adachi

Performance Enhancement of F-PDCH Using Oversampling Diversity MMSE Receive Equalizer 753
Chanho Yoon and Joonhyuk Kang

Control Channel Assisted Chip Equalization for CDMA Downlink Adaptive Modulation and Coding System 758
Arik Gubeskys and Amir Chass

Sparse MAP Equalizers for Turbo Equalizations 762
J. Park and S. B. Gelfand

Indoor/Outdoor Location of Cellular Handsets Based on Received Signal Strength

Jian Zhu
School of Electrical and Computer Engineering
Georgia Institute of Technology
Atlanta, Georgia 30332–0250
Email: jetzhu@ece.gatech.edu

Prof. Gregory D. Durgin
School of Electrical and Computer Engineering
Georgia Institute of Technology
Atlanta, Georgia 30332–0250
Email: durgin@ece.gatech.edu

***Abstract*— This paper demonstrates the feasibility of received signal strength (RSS) methods for locating wireless handset calls in a real cellular environment. An extensive measurement campaign conducted on the Georgia Tech campus indicates that RSS location techniques can locate handset calls within 100 m error distance to its ground truth up to 78% of the time and less than 300 m error distance up to 98% of the time for a network with a majority of *indoor* users. This is well above the safety requirements mandated by FCC in the US. We also propose a Received Signal Strength Aggregate (RSSA) method for identifying and locating *indoor* handsets.**

Keywords- RSS; Radiolocation; Cellular; Propagation

I. Introduction

In recent years, radiolocation technology has received inreasing international attention, particularly in in the United States, where the Federal Communication Commission (FCC) now requires cellular service providers to locate cell phone users within 100 m error distance 67% of the time. TOA [1] , AOA [2] , GPS, and RSS signatures [3] technologies have been developed to provide wireless service providers with more accurate location estimates. Compared with most other cellular location solutions, a RSS location methohd does not require expensive base station equipment, has faster deployment speed, and covers current and legacy handsets making it a low-cost solution for emerging location-based services across the world.

The RSS technique estimates a cellular phone's location by matching signal strengths measured at the handset with signal strengths recorded in a database of radio frequency (RF) maps. These RF maps are generated through a combination of propagation modeling and field measurement. The technique has found its most common application in indoor wireless local area data networks [4]. Laitinen, et. al. in [5] report location performance statistics for *outdoor* users in a GSM network, but there has been no previous research that includes *indoor* users – which now constitute the bulk of today's cellular network traffic.

In this paper, we demonstrate the viability of Received Signal Strength (RSS) techniques in a semi-urban environment to meet the safety requirements set forth by the Federal Communications Commission (FCC). Furthermore, we conclusively show that RSS location techniques are also accurate for indoor users – a characteristic unique among all currently proposed E911 technologies. Since most cellular phone calls are now placed from indoor environments, this result has enormous implications for public safety. We also show that the RSS technique can discriminate between indoor/outdoor users with up to 94% reliability. Results from an IS-136 network in Atlanta Georgia show that the proposed method can locate outdoor users within 100 m 74% of the time and 300 m 97% of the time when only 6-sector information is available. When the system is loaded with indoor users, the accuracy falls to 70% of the time within 100 m and 96% of the time within 300 m. Three different databases of RF maps were compared side by side so that the accuracy effects of different ratios of RF modeling and measurement can be seen.

II. Experiment Environment

Tests were performed on an 850 MHz IS-136 cellular network in mid-town Atlanta on the campus of the Georgia Institute of Technology. The campus approximates a typical semi-urban or dense suburban area with streets, moderate green space, and many 4-5 story academic and office buildings. There are no skyscrapers or "urban canyons" that would be associated with dense urban environments. The measurement area has length of 700m and width of 500m, as shown in Fig. 1. Three base stations were inside the measurement area, where eight medium-tier sectors are in use. Another five base stations in the neighborhood also provided coverage at the edge of the test area. The distance between base stations was approximately 400-500 meters. A database of RF coverage maps for all nearby serving sectors was created from a combination of propagation modeling and varying levels of indoor and outdoor measurement calibration using a Comarco IS-136 scanner with baseband decoding. Real pedestrian-style handset measurements were taken with an Ericsson handset connected to an Ericsson TEMs data collection unit.

This measurement campaign lasted for 4 months (January through April) in the beginning of 2004. Due to the limitations of GPS, many outdoor coordinates and all indoor coordinates had to be painstakingly estimated from geo-referenced maps of campus and manually entered into the database. This is one source of error in our measurements. There are other unique sources of error in our measurements that may make our results somewhat pessimistic. For example, there was a

0-7803-8887-9/05/$20.00 ©2005 IEEE

This material may be protected by Copyright law (Title 17 U.S. Code)

Fig. 1. Satellite photograph of the indoor/outdoor "radiolocation laboratory" at Georgia Tech campus in semi-urban Atlanta, GA.

seasonal change in the middle of our data collections where leaves grew back on the campus trees, changing the propagation characteristics by several dB. Also, one of the large buildings within our test area was demolished in the middle of our campaign. We also used a fairly simple location algorithm since we were concentrating on the more complicated question of indoor feasibility. There are many other algorithms that have been proposed which could improve the performance [5], [6], [7].

III. RSS Location System

A. How RSSI-based Radiolocation Works

The operation of RSSI-based position location is straightforward. A cellular network area is represented in a computer by a large, two-dimensional raster array with uniform grid spacings of 10m squares. Each raster point in the grid corresponds to a location within the network and contains a vector of received signal strength indicator (RSSI) values in dBm for all audible base stations. A complete raster array of RSSI is called an RF Map Database (RFMD). Once an RFMD has been constructed for a network area, the RSSI-based location engine must compare received signal strength measurements made by the handset to the RFMD vectors. The best match determines the xy-coordinates of the most likely handset location.

B. Calibration Level of RF Map Database:

The database used in the location experiments is a collection of raster-based RF maps (10m by 10m resolution). The basic propagation prediction technique used to make the initial RF maps. All pure signal strength predictions are based on a modified version of the Hata model [8]. The radio link budget used for this type of link is given below:

$$P_R = P_T + G_R + G_T \cos(\theta - \theta_b) - 10n \log_{10}\left(\frac{d}{1\text{ m}}\right) - 20\log_{10}\left(\frac{4\pi}{\lambda}\right) + C_{\text{dB}} \quad (1)$$

where the terms in Equation 1 are summarized as follows:

P_R	-	power received by a handset (dBm)
P_T	-	power transmitted by a sector (dBm)
G_R	-	estimated handset antenna gain (0 dBi)
G_T	-	estimated peak sector antenna gain (7 dBi)
θ	-	bearing angle of predicted location (degrees)
θ_b	-	sector antenna bearing angle (degrees)
d	-	separation distance (m)
n	-	path loss exponent (3.3)
λ	-	wavelength of radiation (m)
C_{dB}	-	constant offset (dB)

In this manner, we construct every raster RF map at 10m × 10m resolution for each sector in and around the campus of Georgia Tech. A modeled estimate of signal strength, P_R, is placed at every raster point in an RF map.

Then the modeled RF maps are compared to any available scanner measurements, which are also grouped into 10m by 10m rasters with linear power averaging to remove small-scale fading effects. The variable C_{dB} in Equation 1 is the constant offset term that accounts for additional gains and losses due to antenna height and pattern, RF hardware, frequency offset, or any other consistent, unmodeled effects in the RF chain. The value for C_{dB} is chosen to minimize the standard deviation error between the raw modeling and any drive test measurements corresponding to the sector. It can be expressed in the following Equations. Let vector $a = D_{rss}(x_i, y_i)\ i = 1 \ldots M_n$ denotes driving test RSS measurement, where (x, y) are the coordinate of the i-th measurement point and M_n is the total measurement number. Let vector $b = RFMD(x_j, y_j)$ denotes the RSS of the same dedicate control channel (DCCH) in RFMD.

$$\begin{aligned} C_{\text{dB}} &= (i^T \cdot i)^{-1} \cdot i^T \cdot (b - a) \\ &= \frac{1}{M_n} \sum_{i=1}^{M_n} (D_{rss}(x_i, y_i - RFMD(x_i, y_i))) \quad (2) \end{aligned}$$

where $i = [1, 1, ..., 1]^T$ of $1 \times M_n$

In map areas that are far from measured points, we are forced to rely on purely modeled signal strength. For areas in an RF map that are several raster points away from measured data points, we use a weighted combination of the modeled values and the value of nearby measurement point. This process of blending modeled signal strength with nearby measurements is called *local interpolation*. Thus, each RF map contains scanner measurements which gracefully blend into modeled, unmeasured regions.

There are many imaginable schemes for local interpolation. The scheme used in our RF maps is a 2D cubic interpolation scheme over a diamond-shaped area that surrounds every measured raster point. The difference between measured, interpolated, and modeled signal strength regions is illustrated in Figure 2. Enlarging the radius of the diamond around each measurement point leads to more aggressive interpolation. All RF maps in this study use interpolation with a radius of 3 raster points (30 meters) from measurement center.

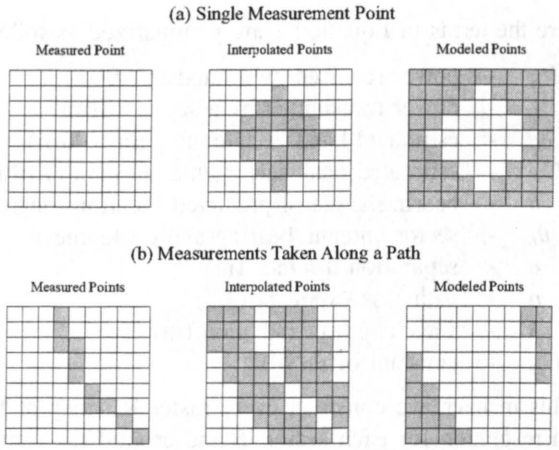

Fig. 2. Marked raster regions (in gray) for (a) a single measurement and (b) a path of measurements.

It should be noted that most measured points do not occur in isolated regions as illustrated in the upper part of Figure 2. Measured data points tend to cluster along paths due to the walking or driving methods of collection. For this reason, the lower part of Figure 2 represents a more realistic separation of interpolation regions. For clusters or paths of measured points, the diamond-shaped interpolation region are cumulatively masked together for every single collected point.

Also note that each measured point is actually the linear average of every instantaneous RF scanner measurement made at a frequency whose longitude and latitude happen to fall within the 10m × 10m raster point. This effectively removes any small-scale fading effects or other anomalies in the collection procedure. Drive-test measured points typically have 3 to 5 instantaneous power measurements averaged within a single raster point. Pedestrian collections typically have 5 to 15 (or more) averaged power measurements due to the slower collection speed.

Our study reports location performance using 3 different levels of RF map database. The Level 1 database of RF maps is calibrated with only outdoor drive-test scanner measurements. The Level 2 database of RF maps is identical to the Level 1 database of RF maps, except raster points corresponding to indoor locations are modified with additional penetration loss based on a simple, georeferenced map of building footprints. The Level 3 database of RF maps is constructed from extensive outdoor *and* indoor measurements. Figure 3 is one example measured at architecture building. Due to the difficulties, time, and expense of taking indoor measurements in every building, the Level 3 database of RF maps may not be practical for widespread deployment. But the Level 3 database does show the upper-limit of performance for an indoor/outdoor location algorithm.

C. Handset RSS Properties:

The additional penetration losses experienced by indoor cellular users were large enough to reliably distinguish them from the outdoor users. Accurate distributions of RSS from indoor

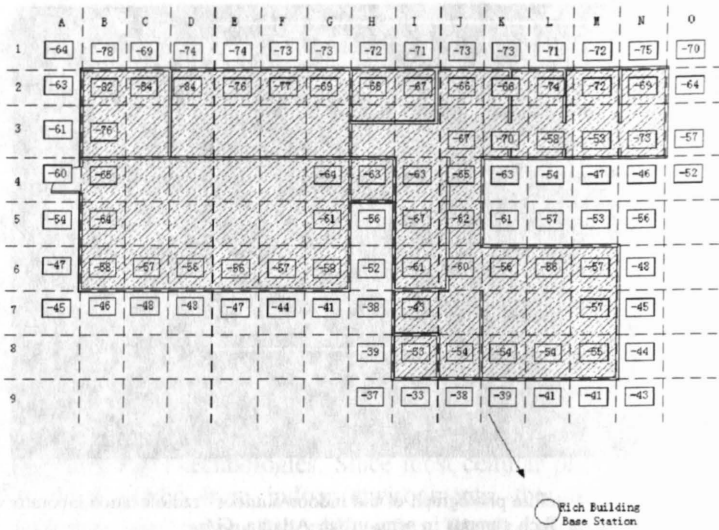

Fig. 3. Measured received signal strength of the architecture building at Georgia Tech. (in dBm)

and outdoor callers can be used to calculate from where a call originates. Based on these handset measurements, the average RSS over the N strongest channels was calculated, which we call the *received signal strength aggregate* (RSSA_N). We can assume that the distributions of the six strongest channels are independent and that their dB-sum is log-normal distributed. Based on our experiment, the mean of indoor RSSA_6 is -97.8 dBm and the standard deviation is 14.1 dB. For outdoor RSSA_6, the mean is -85.5 dBm and the standard deviation is 9.7 dB. Thus, average penetration loss is 12.3 dB. The probability density function of indoor and outdoor RSSA_6 is shown in Equation 3 and 4, respectively. Figure 4 shows the distribution of RSSA between indoor calls and outdoor calls in side-by-side plots.

$$p_{i6}(x) = \frac{1}{14.1\sqrt{2\pi}} e^{\frac{-(x-(-97.8))^2}{(2*198.81)}} \quad (3)$$

$$p_{o6}(x) = \frac{1}{9.7\sqrt{2\pi}} e^{\frac{-(x-(-85.5))^2}{(2*94.09)}} \quad (4)$$

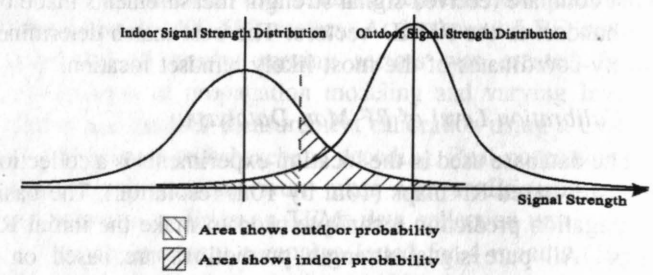

Fig. 4. Lognormal distributions for Indoor and outdoor RSSA.

D. Location Algorithm

The inputs to the location algorithm are a calibrated RFMD and a sequence of NMRs. After normalizing the RSS vector

from NMR and RSS vector at each raster point of RFMD, Euclidean distances between the vectors are calculated. Indoor/Outdoor decision is used to weight the Euclidean distance. The location estimation is the coordinates pair (x, y) with the lowest weighted Euclidean distance.

A handset NMR that contains N received signal strength measurements is like a point in N-dimensional space. The RSS of each control channels is one dimension in the N-dimensional space. This is also true for the collection of signal strengths in a RFMD. Each physical xy location modeled in the Georgia Tech campus RFMDs contains up to 26 received signal strength values, each corresponding to different IS-136 800 MHz control channels. From these values, a location algorithm selects a subset of N values that corresponds to the same control channels present in the NMR. Thus, we need a general formula for calculating the matching distance between two N-length vectors of received signal strength.

If an NMR reports signal strengths from N control channels, then we may represent this measurement as a vector of length N:

$$[Nrss_{i,1}\ Nrss_{i,2}\ \cdots\ Nrss_{i,N}] \tag{5}$$

where $Nrss_{i,j}$ is the ith reported signal strength of the jth control channel. Likewise, we may construct a similar vector for each discrete (x, y) location in the RFMD:

$$[Prss_{x,y,1}\ Prss_{x,y,2}\ \cdots\ Prss_{x,y,N}] \tag{6}$$

where $Prss_{x,y,i}$ is the predicted signal strength of the ith control channel at the xy coordinate.

The steps of the location algorithm are listed below:

1) Linearly average a sequence of 10 NMRs

$$Nrss_j = \sum_{i=1}^{10} Nrss_{i,j} \text{ for } j = 1 \ldots N \tag{7}$$

2) Normalize the averaged-NMR vector by subtracting out the average dBm-power of all received channels to generate the relative received signal strength of the handset measurement Phr_j:

$$Phr_j = Nrss_j - \frac{1}{N}\sum_{i=1}^{N} Nrss_i \tag{8}$$

3) For each raster point in the RFMD, the vector is subtracted out the average dBm-power of the same set of received channels to generate $[Pnr_{x,y,1}\ Pnr_{x,y,2}\ \cdots\ Pnr_{x,y,N}]$:

$$Pnr_{x,y,i} = Pd_{x,y,i} - \frac{1}{N}\sum_{j=1}^{N} Pd_{x,y,j} \tag{9}$$

4) Calculate the Euclidean distance, $M(x, y)$, between these normalized NMR vector and database signal strengths

$$M(x,y) = \sqrt{\sum_{i=1}^{N}(Pnr_{x,y,i} - Phr_i)^2} \tag{10}$$

The xy-coordinate that corresponds to the minimum in M is the pre-estimate for the handset's location.

5) To further improve our location estimation, incorporate our pre-estimate above with indoor/ourdoor discrimination information. Calculate the RSSA_N.

$$x = \frac{1}{N}\sum_{i=1}^{N} Phr_i \tag{11}$$

Calculate the indoor weight factor, which is the area marked with "/" in Figure 4 based on RSSA. The indoor weight factor is the probability that indoor RSSA_N is greater than a value x in the indoor distribution.

Let μ_i denote the mean of RSSA_N for an indoor handset and let σ_i denote the indoor standard deviation of RSSA_N. Then the probability that the handset is indoor is given by Equation 12.

$$\begin{aligned} P_{Ni}(x) &= \frac{1}{\sigma_i\sqrt{2\pi}}\int_{x}^{-\infty} e^{\frac{-(x-\mu_i)^2}{(2\sigma_i^2)}}dx' \\ &= \frac{1}{2}\left(1 - \text{erf}(\frac{x-\mu_i}{\sigma_i\sqrt{2}})\right) \end{aligned} \tag{12}$$

Calculate the outdoor weight factor, which is the area marked with "\" in Figure4 based on RSSA.. The outdoor weight factor is the probability that the outdoor RSSA_N is less than a value x in the outdoor distribution. Let μ_o denote the mean of RSSA_N for outdoor handsets and let σ_o denote the outdoor standard deviation of RSSA_N. Then the probability that the handset is Outdoor is given by Equation 13.

$$\begin{aligned} P_{No}(x) &= \frac{1}{\sigma_o\sqrt{2\pi}}\int_{-\infty}^{x} e^{\frac{-(x-\mu_o)^2}{(2\sigma_o^2)}}dx' \\ &= \frac{1}{2}\left(1 + \text{erf}(\frac{x-\mu_o}{\sigma_o\sqrt{2}})\right) \end{aligned} \tag{13}$$

6) Weighting the distances, $M(x, y)$, by dividing $M(x, y)$ by the indoor/outdoor weight factor as in Equ. 12 or Equ. 13 accordingly which is depended on whether the raster falls within the indoor footprint. If the raster point (x,y) is indoors:

$$M_H(x,y) = M(x,y)/P_{Ni}\left(\frac{1}{N}\sum_{i=1}^{N} Phr_i\right) \tag{14}$$

If (x,y) is an outdoor point:

$$M_H(x,y) = M(x,y)/P_{No}\left(\frac{1}{N}\sum_{i=1}^{N} Phr_i\right) \tag{15}$$

7) Finally, Choose the coordinates x, y with the lowest weighted matching distance to be the location estimation

$$x_m, y_m = Arg\,(Min\,(M_H(x_i, y_j))) \tag{16}$$

TABLE I
LOCATION PERFORMANCE OF RSS LOCATION METHOD.

	Indoor/Outdoor Discrimination Rate					
	M8	M8A	M6	M6A	O6	O6A
LVL1	90%	92%	86%	87%	90%	93%
LVL2	90%	92%	86%	87%	91%	93%
LVL3	90%	91%	87%	87%	89%	94%
	Location Error Statistics— % error < 100 m					
LVL1	56%	61%	52%	62%	54%	68%
LVL2	56%	64%	53%	63%	54%	68%
LVL3	65%	78%	57%	70%	56%	74%
	Location Error Statistics— % error < 300 m					
LVL1	96%	97%	93%	96%	93%	97%
LVL2	96%	98%	93%	96%	93%	97%
LVL3	96%	98%	93%	96%	94%	97%

Lvl1: RF database calibrated with outdoor measurement
Lvl2: Calibration with outdoor measurement and Indoor modeling
Lvl3: Calibration with exhaustive outdoor and indoor measurements
M: Mixed indoor/outdoor sample point (2/3 indoor points)
O: Trial includes only outdoor handsets
8/6: 8- or 6-sector information available
A: Linear averaging of 10 consecutive NMRs

IV. *Results and Discussion:*

A. *Results*

Table I shows results of various location algorithms operating with different types of RF map databases. The linear averaging of 10 consecutive NMRs is very effective in improving the location error statistics, raising the 100 m accuracy numbers between 5% and 18%. With averaging, the performance of the 8-sector cases is almost identical to the performance of the 6-sector cases. This suggests that the strongest 6 received signals contribute the bulk of accuracy to the overall system performance.

An experiments with maps calibrated from only outdoor data is compared with mixed sample point experiment. For 100m-location error statistics, the outdoor test case (O6) is only 6% better than the indoor/outdoor case (M6). This result shows very little degradation and suggests RSS location performance is consistent for indoor and outdoor cases.

B. *Conclusion*

The results in this study demonstrate the feasibility of RSS location techniques for satisfying FCC's requirement. The techniques remain accurate even when the majority of test data is from *indoor* handsets. Since most of today's cell phone calls are placed indoors, inclusion of the indoor data in the evaluation are absolute necessary. Although indoor radio wave propagation losses degrade the performance slightly, the accuracy of the RSS location method can be further improved by using advanced indoor modeling, calibrating RF maps with indoor measurement, and more a complex location algorithm.

Another unique ability of an RSS location technique is the particularly powerful feature for locating and discriminating indoor users, which is unlikely for other triangulation techniques. This could prove to be a very important additional piece of information when dispatching help to the scene of an emergency.

Although the results were developed on a live IS-136 cellular network at 850MHz, the performance is likely similar to other cellular telephony air interface (such as GSM, CDMA, WCDMA, etc.)

C. *Future work*

This paper mainly discusses the feasibility of received signal strength (RSS) methods for locating wireless handset calls in a complicated cellular *indoor* environment. There are more commercial applications (location-based services) that need more accurate location information. To further improve the location accuracy, filtering techniques can be used to give a much better location estimation than the direct averaging method used in this paper.

Another direction for future work is accurate propagation modeling and measurement, which enhance location performance regardless of air interface. Propagation modeling will be increasingly important as RSS location system are deployed. Accurate propagation models reduces the time and cost of extensive drive-tests and also catch modifications to coverage when the cellular network undergoes optimization or build out. Good propagation practice undergirds this entire technology.

REFERENCES

[1] J. Jr. Caffery, "A new approach to the geometry of toa location," *Vehicular Technology Conference, 2000*, vol. 4, pp. 1943 – 1949, 2000.

[2] R. Klukas and M. Fattouche, "Line-of-sight Angle of Arrival Estimation in The Outdoor Multipath Environment," *Vehicular Technology, IEEE Transactions on*, vol. 47, no. 1, pp. 342 – 351, Feb 1998.

[3] A.J. Weiss, "On The Accuracy of A Cellular Location System Based on RSS Measurements," *IEEE Transactions on Vehicular Technology*, vol. 52, no. 6, pp. 1508 – 1518, Nov 2003.

[4] Kaveh Pahlavan and Juha-Pekka Mäkelä Xinrong Li, "Indoor Geolocation Science and Technology," *IEEE Communications Magazine*, vol. 40, no. 2, pp. 112–118, Feb 2002.

[5] H. Laitinen, J. Lahteenmaki, and T. Nordstrom, "Database Correlation Method For GSM Location," *Vehicular Technology Conference 2001 Spring. IEEE VTS 53rd*, vol. 4, pp. 2504 – 2508, May 2001.

[6] M. Aso, T. Saikawa, and T. Hattori, "Mobile Station Location Estimation Using The Maximum Likelihood Method in Sector Cell Systems," in *Vehicular Technology Conference 2002-Fall. Proceedings. IEEE 56th*, Sept 2000, vol. 2, pp. 1192 – 1196.

[7] L. Perez-Breva, C.-Y. Chong, R. M. Dressler, P. R. Rao, P. Siccardo, and D. S. Spain, "Location and Determination Using RF Fingerprinting," *U.S. Patent No. 6,393,294, 22 Issued to Polaris Wireless Inc.*, March 2000.

[8] T.S. Rappaport, *Wireless Communications: Principles and Practice*, Prentice-Hall Inc., New Jersey, 2nd edition, 2002.